

The influence of grafting on flow-induced crystallization and rheological properties of poly(ϵ -caprolactone)/cellulose nanocrystal nanocomposites

Maria Eriksson, Anne-Lise Goffin, Philippe Dubois, Ton Peijs & Han Goossens

To cite this article: Maria Eriksson, Anne-Lise Goffin, Philippe Dubois, Ton Peijs & Han Goossens (2018): The influence of grafting on flow-induced crystallization and rheological properties of poly(ϵ -caprolactone)/cellulose nanocrystal nanocomposites, *Nanocomposites*, DOI: [10.1080/20550324.2018.1529713](https://doi.org/10.1080/20550324.2018.1529713)

To link to this article: <https://doi.org/10.1080/20550324.2018.1529713>



© 2018 The Author(s). Published by Informa UK Limited, trading as Taylor & Francis Group.



Published online: 08 Nov 2018.



Submit your article to this journal [↗](#)



Article views: 16



View Crossmark data [↗](#)

The influence of grafting on flow-induced crystallization and rheological properties of poly(ϵ -caprolactone)/cellulose nanocrystal nanocomposites

Maria Eriksson^a, Anne-Lise Goffin^b, Philippe Dubois^b, Ton Peijs^c and Han Goossens^d

^aLaboratory of Polymer Materials, Department of Chemical Engineering and Chemistry, Eindhoven University of Technology, Eindhoven, The Netherlands; ^bLaboratory of Polymeric and Composite Materials, Center of Innovation and Research in Materials and Polymers (CIRMAP), University of Mons, Mons, Belgium; ^cSchool of Engineering and Materials Science, and Materials Research Institute, Queen Mary University of London, London, UK; ^dSabic Innovative Plastics, Bergen op Zoom, The Netherlands

ABSTRACT

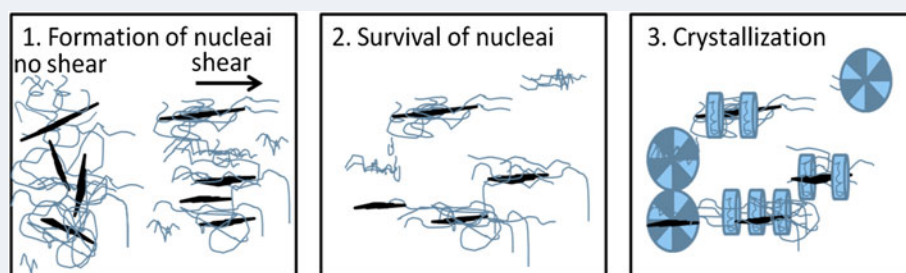
The influence of poly(ϵ -caprolactone) (PCL) grafts on the rheology and crystallization behavior of nanocomposites based on PCL and cellulose nanocrystals (CNC) both under quiescent and shear conditions is investigated. Under quiescent conditions, the grafted nanocrystals have high nucleation efficiencies. Under the influence of shear, the non-grafted nanocrystals were, however, more efficient in orienting the polymer chains and accelerating the flow-induced crystallization. The addition of large amounts of grafted material decreases the viscosity of the composites and thereby also the efficiency of shear-induced orientation.

ARTICLE HISTORY

Received 14 May 2018
Accepted 24 September 2018

KEYWORDS



Poly(ϵ -caprolactone);
cellulose nanocrystals;
grafting; flow-induced
crystallization; SAXS



1. Introduction

Poly(ϵ -caprolactone) (PCL) is an interesting biocompatible and biodegradable polymer, but so far the number of applications has been limited because of its low modulus. Therefore, the potential of many reinforcing fillers has been investigated for its use in PCL-based nanocomposites. In particular, high-aspect ratio fillers such as nanoclays [1–6] carbon nanotubes [1], chitin nanocrystals [7] and cellulose-based crystals [8–13] have shown to improve the mechanical properties of PCL. The use of cellulose-based filler materials is particularly interesting when combined with polymers like PCL or PLA since the resulting composites are fully biodegradable. However, since the macroscopic properties of semi-crystalline polymers such as PCL are largely determined by their morphology, it is also essential to understand the role of these fillers on the crystallization behavior of the polymer in relation to the state of dispersion. It is well known that nanoparticles

can act as nucleation agents and, as such, can change the crystallization kinetics and crystalline morphology of a semi-crystalline polymer [14]. This was also shown for both isothermally crystallized PCL, for which the half time of crystallization was decreased by several minutes, and for continuously cooled PCL, for which the crystallization temperature significantly increased [13,15–20]. One of the most prominent examples is carbon nanotube-filled PCL with an increased crystallization temperature of 14 °C [16,17] and a decreased half time of crystallization at 44 °C from 10.1 min for neat PCL to 1.4 min for a composite incorporating 1.0 wt% multiwalled carbon nanotubes [19]. However, in industrially relevant processes polymers are generally not crystallized under quiescent conditions but exposed to complex flow fields. It has been shown that low shear conditions, i.e. low shear rates and low total shear, increase the crystallization rate by inducing a large number of point-like nuclei, leading to more

CONTACT Ton Peijs  t.peijs@qmul.ac.uk  School of Engineering and Materials Science, and Materials Research Institute, Queen Mary University of London, Mile End Road, E1 4NS London, UK.

© 2018 The Author(s). Published by Informa UK Limited, trading as Taylor & Francis Group.

This is an Open Access article distributed under the terms of the Creative Commons Attribution License (<http://creativecommons.org/licenses/by/4.0/>), which permits unrestricted use, distribution, and reproduction in any medium, provided the original work is properly cited.

homogeneous nucleation while at high shear conditions not only the crystallization kinetics but also the final morphology is altered [21,22]. Moreover, it was shown that low shear has less effect on nucleation in polymer nanocomposites than on the polymer itself, since the nanofiller itself acts as a nucleating agent, inducing more nucleation sites. Crystallization kinetics and crystalline structures obtained under quiescent and flow-induced crystallization in low shear fields are therefore often not too dissimilar. However, in the case of strong shear fields in combination with high-aspect ratio fillers, the fillers are more prone to orient in the direction of the shear field and can thereby provide templates for oriented shish-kebab type crystalline structures. Flow-induced crystallization in polymer nanocomposites is therefore a complex process because several different processes compete. Moreover, the applied shear can also affect the morphology of the filler itself by breaking up of agglomerates and inducing orientation into the system that complicates the overall picture even more.

A common problem in polymer nanocomposites is related to dispersion since the small size of nanofillers makes them prone to agglomeration. The dispersion of nanofillers in a polymer matrix is therefore one of the most important parameters to regulate in order to control the final properties of the nanocomposite material. In order to prevent agglomeration, fillers are often grafted with polymer chains that are compatible with the polymer matrix. It has been shown that dispersion depends predominantly on the ratio between the molecular mass of the matrix polymer and the graft length on the filler and that relatively long grafts are a prerequisite for good dispersion [23,24]. Moreover, grafted nanofillers dispersed throughout the matrix have shown good nucleation ability and accelerate the crystallization kinetics both in non-isothermal and isothermal crystallization conditions [9,25].

As mentioned before, high-aspect ratio fillers affect the crystallization kinetics and the final morphology to a larger extent than spherical particles. Both carbon nanotubes and nanoclays are well-studied examples. Another type of filler that has received a lot of interest lately is nanocellulose or cellulose nanocrystals (CNC) [26]. Cellulose is one of the most abundant materials on earth and, being a biodegradable material, it is of great interest as a reinforcement for biopolymers. Cellulose is a semi-crystalline polymer but when it undergoes an acidic hydrolysis the amorphous matrix can be removed and nano-sized needlelike crystals, known as CNC, are obtained. Even though the exact modulus of CNC is unknown, most results, both theoretical and experimental, point to a value between 100

and 160 GPa [26], being similar to that of Kevlar fibers, which indicates that they have great potential to reinforce many low modulus thermoplastics. The aspect ratio of the obtained nanocrystals depends on the origin of the cellulose and the extraction method. Bleached wood pulp, cotton or ramie fibers are common sources [8]. Since an aspect ratio of at least 10–100 is needed in order for this reinforcement to be reasonably efficient [26], one can easily understand that next to the extraction method the final dispersion of the filler in the polymer matrix is of major importance. Like all nano-sized fillers, CNCs tend to agglomerate. The dispersion of the nanocrystals in the polymer matrix is therefore a major problem and, as a consequence, a lot of effort has been put on the surface modification of these nanocrystals.

A commonly used surface modification method is the grafting of polymer chains of the same kind as the matrix to the surface of the nanocrystals [8–10,27,28]. Habibi et al. [8] showed that by performing a ring-opening polymerization of caprolactone in the presence of CNC obtained from ramie fibers they could make PCL grafted nanocrystals. In a subsequent step, these PCL-g-CNC could be mixed into a PCL matrix via a solvent mixing procedure. The stiffness and the tensile strength of the thus obtained composites were drastically improved compared to neat PCL and composites prepared with non-grafted CNC. Goffin et al. [9] studied the melt-blending of PCL-g-CNC with commercial PCL, showing excellent dispersion and enhanced thermo-mechanical and rheological properties. Also Siqueira et al. [13] prepared nanocomposites of PCL and CNC and compared those to the properties of composites prepared using another cellulose-derived filler, i.e. microfibrillated cellulose (MFC). They concluded that grafting improved the dispersion of the nanocrystals in the organic solvent used for the preparation of the nanocomposites. This led to an increase in the overall strength and stiffness of the composites. In their work, the grafted MFC showed a larger improvement in the stiffness than the nanocrystals, which was attributed to enhanced network formation of the more flexible MFC. It is also worth to note that in that study the degree of crystallization and the crystallization temperature were increased in the nanocrystals-filled composites, while they remained unaltered in the MFC system, the reasons for this not completely understood. Lönnberg et al. [11,12] also worked with MFC and grafted PCL chains of different length to the surface in order to determine the influence of graft length on the mechanical properties of the resulting composites. In their work, the stiffness of the composites was improved, while at the same time the elongation

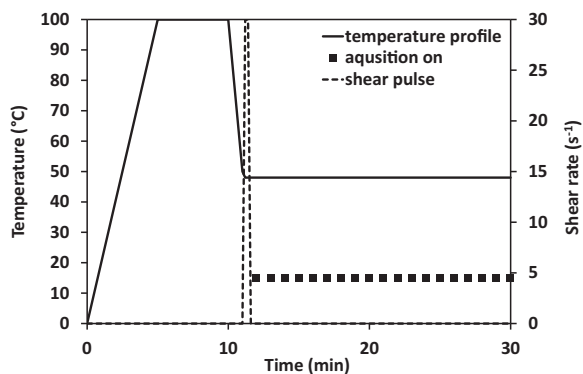


Figure 1. Schematics of the flow-induced crystallization experimental protocol for the in-situ SAXS measurements.

at break was only marginally decreased when a small amount of filler (3 wt%) was added. At higher filler loadings a transition from ductile to a stiff, but brittle material was found.

The objective of this study is to investigate the influence of graft length of PCL-g-CNC on the state of dispersion in a PCL melt and its effect on rheological properties and crystallization behavior of PCL. Both non-isothermal and isothermal crystallization experiments under quiescent condition are performed. In addition, flow-induced crystallization is studied and compared to that of neat PCL.

2. Experimental section

2.1. Materials

PCL CAPA[®] 6400 ($M_n = 40$ kg/mol) from Perstorp Polycaprolactones and PCL from Sigma-Aldrich Co. (St. Louis, MO) ($M_n = 80$ kg/mol) were used as matrix materials. These polymers are further referred to as PCL40 and PCL80, respectively. Three types of CNC, i.e. unmodified, and with short and long grafts (PCL-g-CNC), were prepared. The grafting procedure was described in detail elsewhere [8], but is summarized here. The nanocrystals were obtained after acid hydrolysis of ramie fibers and the grafting of PCL onto the particles was done via a ring-opening polymerization of caprolactone in toluene, catalyzed by a $\text{Sn}(\text{Oct})_2$ catalyst. The graft length was varied by using different reaction times.

2.2. Sample preparation

The composites were prepared in a twin-screw recirculating X'plore 15MC micro-compounder. Seven grams of polymer was premixed with the desired amount of unmodified CNC or PCL-g-CNC and introduced in the extruder operating at a temperature of 150°C and a screw speed of 75 rpm. The materials were mixed for approximately 10 min. Subsequently, the outlet was opened and the extruded fibre strand was cooled to room

temperature (RT). Samples for rheological measurements were pressed in a Dr. Collin hot press. The temperature was set to 100°C, and the samples were first melted for 5 min in a mold between two sheets of aluminum foil and pressed at 100 bars for 2 min. Cooling to RT was performed under pressure.

2.3. Characterization techniques

A TGA Q500 from TA Instruments (New Castle, DE) was used to perform thermogravimetric analysis (TGA) and to evaluate the thermal stability of the grafted nanocrystals and the prepared composites. Ten to 15 mg of sample was heated to 600°C at a rate of 10°C/min under a nitrogen atmosphere. In order to further investigate if degradation takes place during processing, size exclusion chromatography (SEC) measurements were performed. Solutions of 1 mg/mL polymer were prepared in tetrahydrofuran. The molar mass distributions both before and after drying experiments were determined using a gel permeation chromatograph from Waters with a Waters 510 pump and a Water 712 WISP chromatograph with an injection volume of 50 μL . The column used was a PL-gel mix D column from Polymer Laboratories. The molar masses were calculated relative to a PS-standard and are thus not absolute values for PCL. The state of dispersion of the nanocrystals was initially investigated using optical microscopy. Observations were made using a Zeiss Axioplan2 optical microscope equipped with a Zeiss Axiocam camera and a Linkam THMS600 hot-stage for temperature control. In order to obtain more information on the state of dispersion both scanning electron microscopy (SEM) and transmission electron microscopy (TEM) experiments were performed. For SEM imaging the samples were microtomed at -100°C with a glass knife, glued onto a SEM stub and coated with chromium using an Emitech K575X sputter coater (1 min, 100 mA). The state of dispersion of the nanocrystals was also investigated using TEM. Ultrathin sections (70 nm) were microtomed at -100°C using a Leica Ultracut S/FCS microtome. The sections were put on a 200 mesh copper grid with a carbon support layer. The sections were thereafter examined in a Tecnai 20 TEM, operated at 200 kV. Transition temperatures of the nanocomposites were determined via differential scanning calorimetry (DSC) measurements using a Q1000 DSC from TA Instruments. The samples were heated from RT to 100°C at a rate of 10°C/min and held at that temperature for 5 min. Subsequently, the samples were cooled to -80°C also at a rate of 10°C/min and kept at this temperature for 5 min. The cycle was repeated once. The melting, crystallization and glass transition

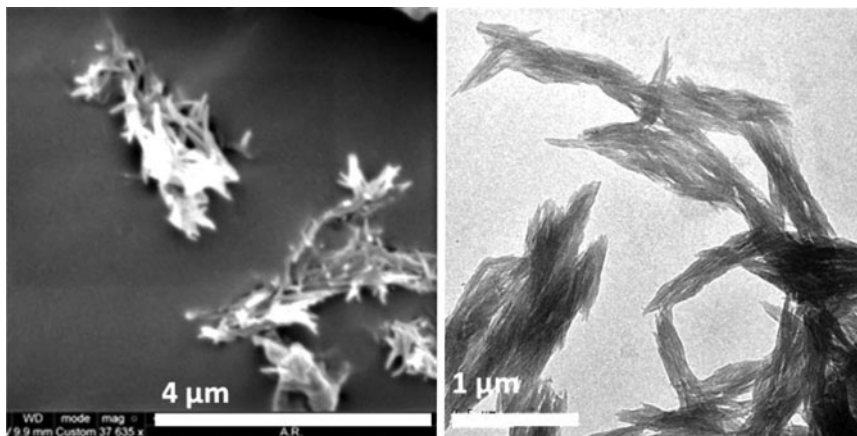


Figure 2. Left: SEM image of grafted CNC, right: TEM image of grafted CNC.

temperatures were determined from the second heating run. The same analysis was also performed on the CNC and PCL-g-CNC prior to preparing the composites. For the isothermal crystallization experiments the samples were initially subjected to two heating/cooling cycles as previously described, followed by heating from RT to 100 °C at a rate of 10 °C/min and held at that temperature for 5 min. Subsequently, the samples were cooled at the maximum cooling rate, i.e. 50 °C/min, to the desired isothermal temperature, at which they were kept for 30 min before heating up to a temperature of 100 °C again. The cycle was repeated for four different isothermal crystallization temperatures.

In-situ crystallization experiments using small-angle X-ray scattering (SAXS) were performed at the Dutch-Belgian Beamline (DUBBLE) beamline at ESRF, Grenoble, France. An energy of 12 keV was used and the sample-to-detector distance was 7 m. A Linkam Optical Shearing System (CSS450) was used for temperature control and the samples were heated to a temperature of 100 °C and kept there for 5 min in order to erase all thermal history. Subsequently, they were cooled with 20 °C/min to a temperature of 48 °C. Upon reaching the isothermal temperature the samples were exposed to a shear pulse of 30 s⁻¹ for 1 or 3 s, and SAXS data acquisition of one frame every 15 s was started. The crystallization behavior of the samples without shear was also recorded. A schematic description of the experiment can be found in Figure 1.

Rheological measurements were performed on a stress-controlled AR-G2 rheometer from TA Instruments under a nitrogen atmosphere. Different methods were used for PCL40 and PCL80. The 40 kg/mol PCL samples were measured by using a 25 mm plate-plate geometry and frequency sweeps were performed at 60 and 100 °C in an angular frequency range of 0.1–100 rad/s with a constant strain of 10%. The 80 kg/mol samples were measured by using an 8 mm plate-plate geometry for frequency

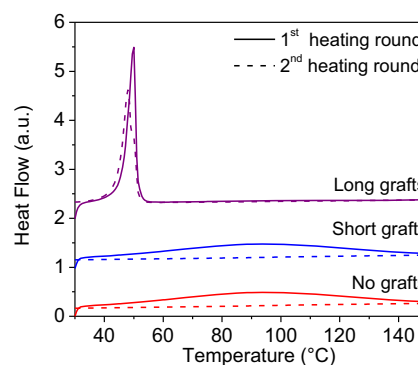


Figure 3. DSC heating traces of CNC and PCL-g-CNC with different surface grafts.

sweeps at 65, 100 and 150 °C and an angular frequency range of 100–0.1 rad/s with a constant strain of 10%.

3. Results and discussion

3.1 Crystallization behavior of PCL/CNC

The PCL grafted nanocrystals (PCL-g-CNC) were obtained as dried powder. In Figure 2 both TEM and SEM pictures of the as-received powder of grafted CNC with long grafts are shown. Large agglomerates of what seem to be loosely attached nanocrystals are observed.

Once the nanocrystals are dispersed in the polymer matrix, it is difficult to assess their state of dispersion. Due to the small difference in contrast between the PCL matrix and CNC, visualization by means of TEM is difficult.

In order to investigate the thermal behavior of the PCL-g-CNC, DSC analysis was performed on the dried powder. Figure 3 shows the heating curves of DSC scans of CNC with different graft lengths. A melting peak can be observed in the sample with longer PCL-grafts. Apparently, these grafts are sufficiently long to crystallize even in the absence of matrix polymer. The short grafted and non-grafted

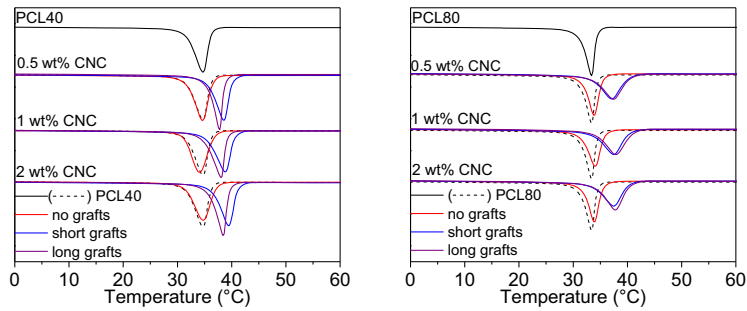


Figure 4. DSC traces of the different PCL/CNC nanocomposites recorded upon cooling. Left: PCL40 matrix, right: PCL80 matrix.

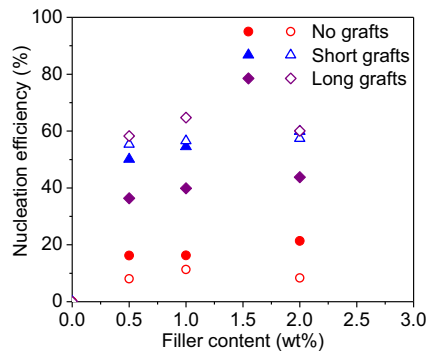


Figure 5. The nucleation efficiency as a function of filler content for the different melt-extruded PCL/CNC nanocomposites. The filled symbols represent the PCL40 matrix and the open symbols represent the PCL80 matrix.

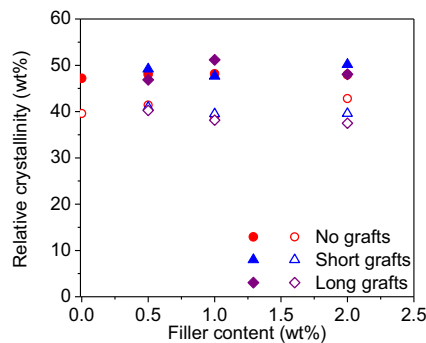


Figure 6. The relative degree of crystallinity as a function of filler content for the different melt-extruded PCL/CNC nanocomposites. The filled symbols represent the PCL40 matrix and the open symbols represent the PCL80 matrix.

nanocrystals show similar DSC traces with no apparent melting peak.

After this initial characterization of the non-grafted and grafted CNCs, the influence of molar mass of the grafts on dispersion quality in the PCL matrix was studied. In Figure 4 the DSC traces recorded during cooling are shown and it is obvious that for both PCL molar masses the surface modified CNCs introduce a significant nucleation effect into the PCL matrix, since all the crystallization peaks are shifted to higher values. From the onset of the crystallization temperature the nucleation efficiency (N.E.) was calculated according to the method described by Fillon et al. [29,30] that is expressed as;

$$N.E. = \frac{T_{c,comp} - T_{c,poly.}}{T_{c,poly,max} - T_{c,poly.}} \cdot 100\% \quad [1]$$

where $T_{c,comp}$ is the onset temperature of the crystallization for the nanocomposite, $T_{c,poly.}$ is the onset temperature of the polymer matrix and $T_{c,poly,max}$ is the crystallization temperature of the self-nucleated polymer. $T_{c,poly,max}$ was determined via self-nucleating experiments performed according to the method described by Fillon et al. and was found to be 45.0 °C and 46.3 °C for PCL40 and PCL80, respectively. In Figure 5 the nucleation efficiencies calculated from the onset of crystallization temperatures are presented. The non-grafted CNC has a very modest nucleation efficiency of around 5–10%, while the efficiency for the PCL-g-CNC is higher than 50% for both matrix materials. The crystallization temperatures in the composites with the PCL-g-CNC are all above 40 °C which is high for PCL and its nanocomposites [16]. It is worthwhile to note that the short grafted nanocrystals show the best nucleation efficiency in PCL40 while in the higher molar mass matrix the long grafted nanocrystals are most efficient. Furthermore, a maximum efficiency at 1 wt% for the higher molar mass matrix is observed while in the lower molar mass matrix the nucleation efficiency is monotonically increased with increasing filler content.

When the values of nucleation efficiency are compared to literature, the nucleation efficiency of the non-grafted CNC in PCL is modest. For carbon nanotubes very high nucleation efficiencies of 200% and above were reported [16,17]. But it has to be mentioned that in these studies extremely low values for the crystallization temperature of neat PCL were used, which could be part of the explanation of these very high nucleation efficiency values. This might be related to the fact that they used PCL directly after synthesis, while we applied an additional extrusion step to make the reference (unfilled) PCL matrix. If we directly compare the onset temperature of crystallization, the values obtained from our experiments are among the highest observed and the nucleation efficiencies of PCL-g-CNC is in the range of carbon nanotubes.

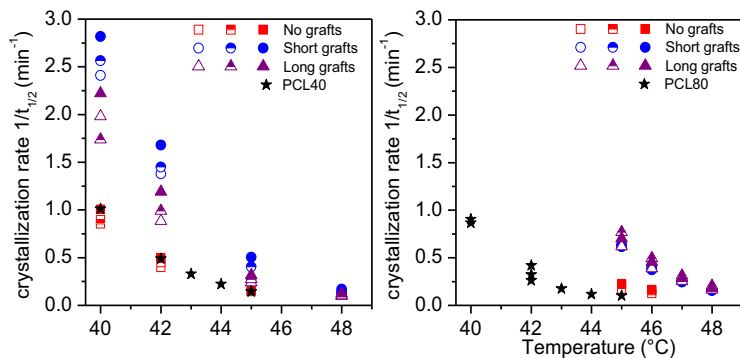


Figure 7. The crystallization rate as a function of temperature for the different PCL/CNC nanocomposites. Left: PCL40 matrix and right: PCL80 matrix. Data for the composites with CNC without grafts are represented by squares, with short grafts by circles and long grafts by triangles. Composites with 0.5 wt% CNC are represented by open symbols, 1 wt% CNC by half filled symbols and 2 wt% CNC by fully filled symbols.

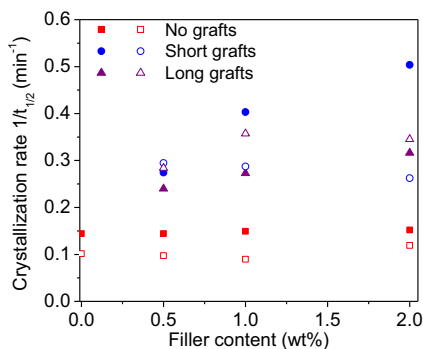


Figure 8. The crystallization rate as a function of filler content for the different PCL/CNC nanocomposites. The isothermal crystallization temperature was 45 °C. The filled symbols correspond to the PCL40 matrix and the open symbols to the PCL80 matrix.

In **Figure 6** the relative degree of crystallinity as calculated from the area under the melting peak of the second heating run is shown. Values of around 48% for PCL40 and around 40% for PCL80 are observed. These values correspond well with earlier reported values for PCL.

In order to gain more insight in the crystallization kinetics of the nanocomposites also isothermal DSC experiments were performed. It should be noted that it was hard to find a temperature range where comparisons could be made between the CNC-filled samples and the reference polymer. The nanocrystals show good nucleation ability and the observed increase in crystallization temperature was several degrees in the non-isothermal experiments. This has implications for the isothermal experiments. At low temperature, i.e. below 42 °C, crystallization in the CNC-filled samples is extremely fast. It does in fact already start during the cooling step to the desired temperature. Therefore, the Avrami analysis performed in this temperature window will contain large errors and the values will not be representative. At too high crystallization temperatures, i.e. 48 °C and higher, the neat polymer does not crystallize within a

realistic timespan. Therefore, we are restricted to a very narrow temperature window of a few degrees where the crystallization rates are comparable. The Avrami analyses were performed on all the crystallization data. In its simplest form the crystallization kinetics can be described by;

$$X(t) = 1 - e^{-K(T) \cdot t^n} \quad [2]$$

where the Avrami parameters n and $K(T)$ can be determined from the slope and the intercept of the linear fitting of $\log(-\ln(1-X(t)))$ versus $\log(t)$ respectively. In accordance with literature, only values between 0.3 and 20% of relative crystallinity were used to determine these parameters. After the values of n and $K(T)$ were obtained, the half time of the crystallization could be calculated via;

$$t_{0.5} = \left[\frac{\ln 2}{n \cdot K(T)} \right]^{\frac{1}{n}} \quad [3]$$

The rate of crystallization can then be described as the inverse of the half time of crystallization. In **Figure 7** the crystallization rates of the different nanocomposites as a function of temperature are presented. As previously mentioned, the data of the CNC-filled samples at lower temperatures (<45 °C) are erroneous and can only be considered as an indication of the crystallization rate. However, what can be observed from these plots is that the addition of PCL-g-CNC greatly influences the crystallization kinetics of PCL. Non-grafted nanocrystals do not increase the crystallization rate in a significant way.

In order to better visualize the influence of the nanofiller, the crystallization rate was plotted versus filler content for a crystallization temperature of 45 °C. These data are presented in **Figure 8**. As already mentioned, the crystallization rate is unaffected by the addition of the non-grafted nanocrystals. The addition of the grafted nanocrystals greatly enhances the crystallization rate, which for the lower molar mass matrix reaches values that are three times higher than for the neat polymer.

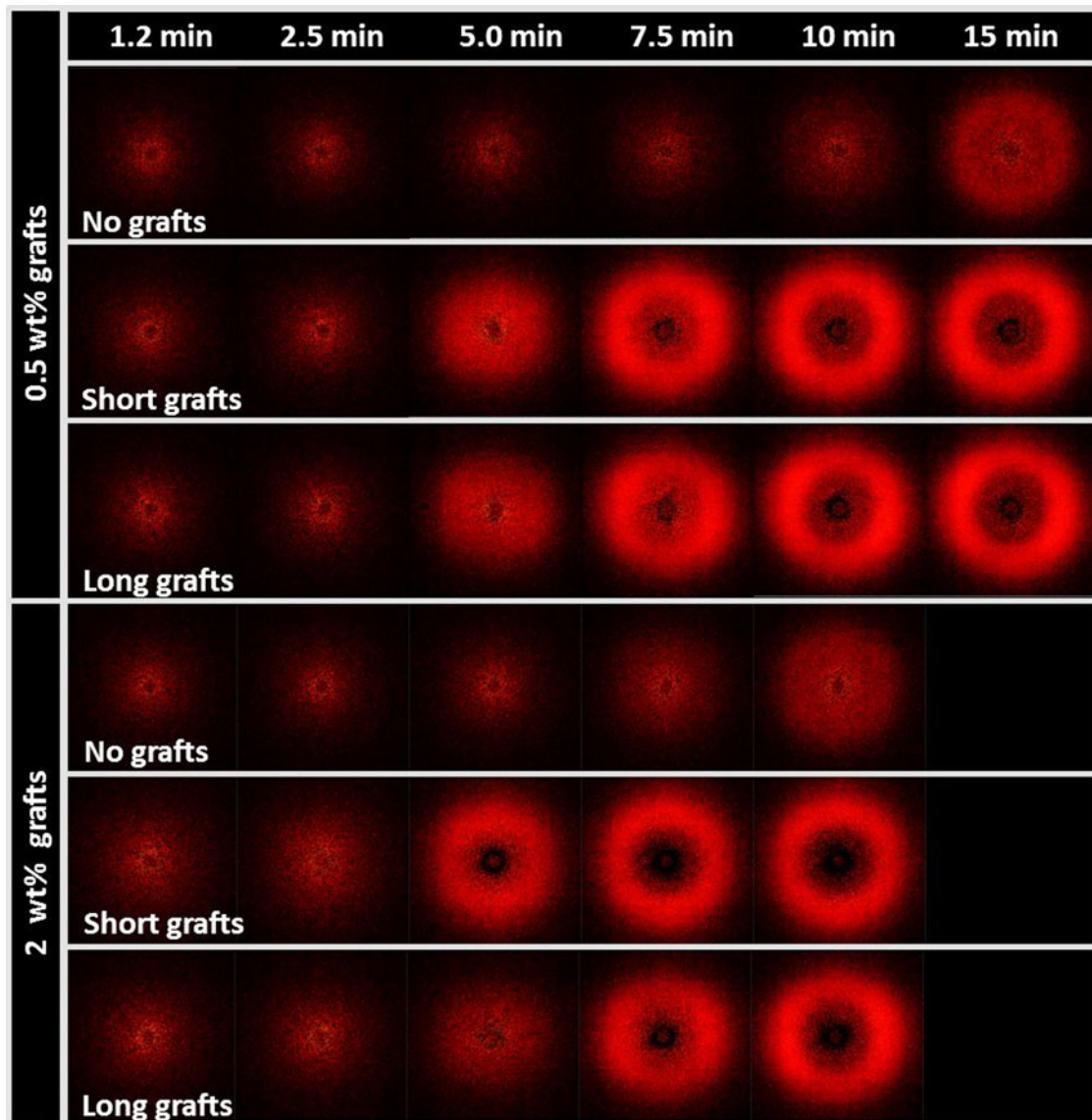


Figure 9. SAXS images obtained during isothermal crystallization of PCL/CNC nanocomposites. The temperature is 48 °C and the molar mass of the PCL matrix is 40 kg/mol.

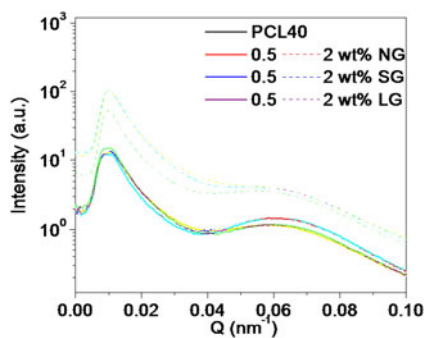


Figure 10. Integrated SAXS patterns of neat PCL and the different PCL/CNC nanocomposites. The last frame of each sample was integrated in order to assure complete development of the structure in each individual sample. The temperature is 48 °C and the molar mass of the PCL matrix is 40 kg/mol.

Similar to the non-isothermal experiments, a maximum value for the higher molar mass matrix is observed, while for the lower molar mass matrix there is a monotonic increase in crystallization rate.

The better performance of nanocrystals with long grafts in a high molar mass matrix and fillers with short grafts in low molar mass matrix is also consistent with the trend from the non-isothermal experiments.

From the DSC results it could be concluded that PCL-g-CNC does not only have a strong nucleation effect on PCL, but that they also greatly influence the kinetics of crystallization, reducing the crystallization time to more than half its value. From in-situ SAXS experiments during isothermal crystallization, the influence on the kinetics of crystallization can also clearly be seen. The isothermal crystallization temperature was set to 48 °C, a temperature at which the crystallization of neat PCL normally takes up to one hour. In **Figure 9**, SAXS images recorded at different times after the isothermal temperature was reached are depicted. These images confirm the results from the DSC experiments and show a remarkable nucleation effect of

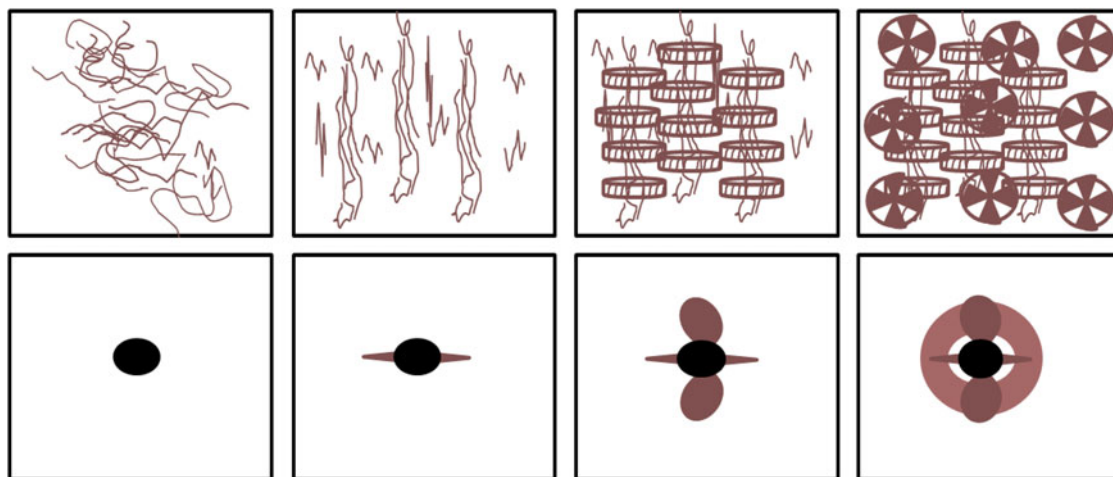


Figure 11. Different steps of crystallization under shear. The top row shows schematics of the structure and the bottom row the corresponding 2D SAXS image. From left to right: unstrained melt; formation of shish; formation of kebabs from the existing shish; growth of spherulites resulting from relaxed row nuclei.

PCL-g-CNC. In the DSC experiments it was also observed that filler addition had little effect on the crystallinity and melting temperature. It is therefore expected that, even though the SAXS experiments show an increased crystallization rate, the structure of the polymer should be unaffected.

The integrated data for the fully crystallized samples are presented in Figure 10. The q -value corresponding to the maximum of the peak around 0.06 nm^{-1} gives information about the long period, which corresponds to the distance between adjacent lamellae. Although filler addition affects the rate of crystallization, the crystalline structure obtained after the isothermal crystallization is similar for all samples and the long period remains constant.

3.2. Shear-induced crystallization behavior of PCL/CNC

During extrusion, compounding and injection molding, polymers are often exposed to high shear forces. As a result of these shear forces the polymer chains tend to align in the flow direction, which facilitates the formation of nuclei [31]. SAXS is a very useful tool for studying structure development in semi-crystalline polymers. In Figure 11, a schematic representation of different SAXS patterns corresponding to different steps of shear-induced crystallization are presented. When the polymer is in its molten state only background scattering is observed. The orientation of polymer chains with the shear flow (vertical in the pictures) gives rise to streaks at the equatorial. The crystallization of lamellae with a preferred direction perpendicular to the flow is represented in the 2D SAXS images as meridional lobes. These two scattering patterns together represent the so-called shish-kebabs. Spherulitic crystallization

from point-like nuclei is characterized by the appearance of an isotropic ring.

With the background information provided by Figure 11, the SAXS patterns obtained in our experiments can now be analyzed. Anisotropic fillers like CNCs, are thought to greatly affect shear-induced crystallization of semi-crystalline polymers. They can both align in the direction of the applied shear pulse, and thereby provide nucleation sites [32], and change the relaxation behavior of the polymer matrix in the melt. In order to exploit this behavior, the shear-induced crystallization of the composites was studied using in-situ SAXS experiments. The experiments were set up similarly to the isothermal experiments presented in the section above with the difference that a shear pulse was applied once the isothermal temperature was reached. In a first step the shear-induced crystallization of neat PCL was investigated. Results from experiments with a shear pulse of 60 s^{-1} with different durations are presented in Figure 12.

The application of a shear force gives rise to a very different structure as compared to the isothermally crystallized samples. First, the formation of oriented structures is observed, characterized by the lobes at the meridional which are later overgrown by non-oriented structures (isotropic ring) in the latter stages of crystallization. When the shear rate is increased the ratio of oriented over spherulitic crystals is increased and at the longest shear pulse only oriented crystals are observed, even though the molar mass is rather low in the case of the PCL40 matrix. In the PCL80 based samples of higher molar mass the rate of crystallization is increased and the amount of both spherulitic and oriented structures is increased as compared to the lower molar mass PCL40 matrix at the same shear time.

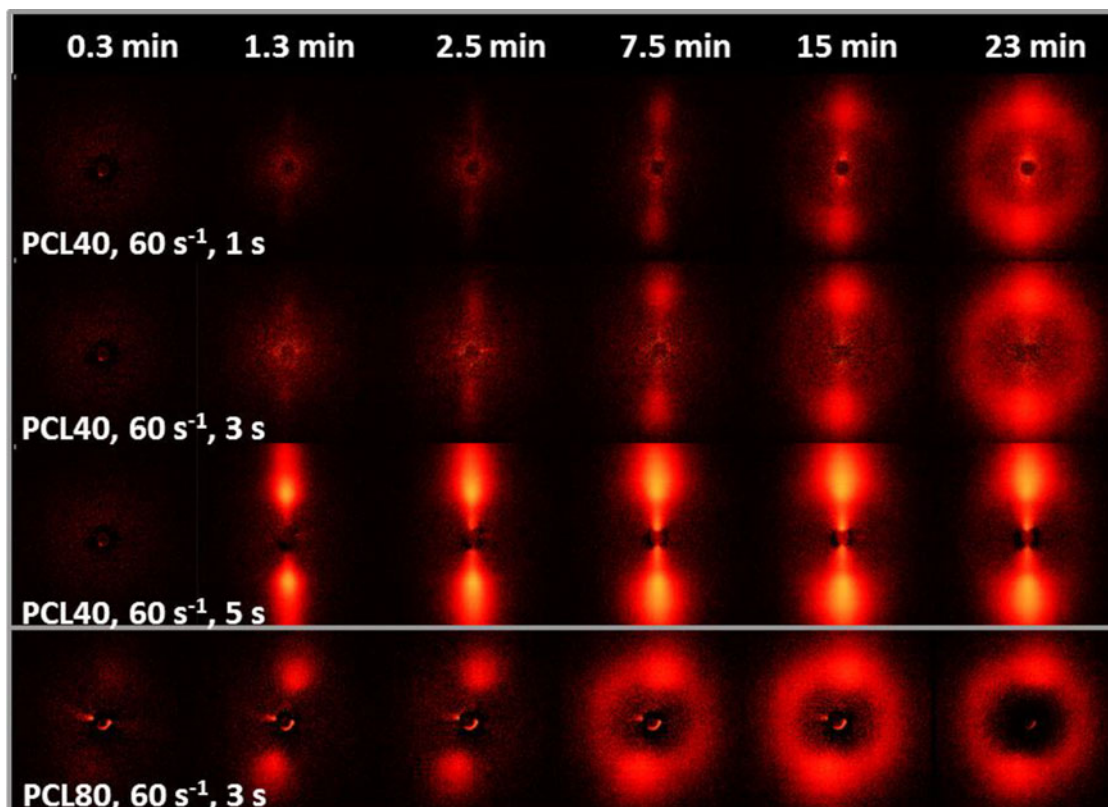


Figure 12. SAXS images obtained during shear-induced crystallization of unfilled PCL. The temperature is 48 °C and the molar mass of the PCL matrix is 40 kg/mol for the top three rows and 80 kg/mol for the bottom row. The shear rate is 60 s^{-1} and the lengths of the pulses were 1, 3 or 5 s.

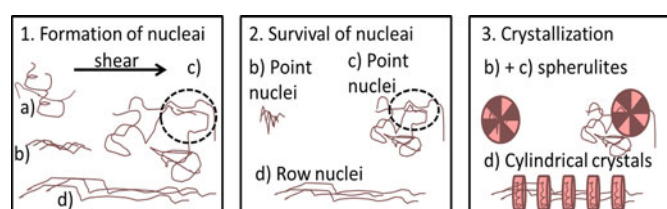


Figure 13. Schematic of shear-induced crystallization. Different cases are depicted. (a) low molar mass and weak flow; (b) low molar mass and strong flow; (c) high molar mass and weak flow; and (d) high molar mass and strong flow.

Based on this observation the shear-induced crystallization of PCL can be explained. The crystallization process under shear can be divided into three stages: (i) formation of nucleus under the influence of shear, (ii) survival of the nucleus once the shear is ceased and (iii) the final crystallization step [33,34]. This is schematically depicted for an unfilled polymer in Figure 13. Higher molar mass polymers are in general easier to align than lower molar mass polymers, due to their higher viscosity and the development of higher shear forces at the same applied shear. Once shear is ceased, the survival of the nuclei depends on the relaxation time of the polymer [31]. Lower molar mass polymers tend to have very short relaxation times and the probability that nuclei will survive is very low. Even if the polymer was fully oriented during the shear step, the orientation can be relaxed and a point-like nucleus will be formed. In the subsequent crystallization step these nuclei will be the starting point

of the formation of spherulitic structures. If the orientation of the chains is preserved, row nuclei are formed. From the row nuclei cylindrical crystals with a long period L will grow with lamellae that are perpendicular to the flow direction.

Based on this schematic picture the results for the neat PCL can be explained. In both matrices the formation of oriented structures is observed, indicating that even in the lower molecular weight PCL40 the relaxation time of the polymer chains is long compared to the crystallization rate, allowing for the survival of nuclei and crystallization prior to the relaxation of the orientation provided by the shear pulse. Increasing the shear time leads to an increased orientation of the polymer chains and at a shear time of 5 s almost all the lamellae in the PCL40 matrix appear to be oriented perpendicular to the shear field. There are no signs of streaks at the equatorial, which are characteristic for shish formation. The fact that these streaks can not be

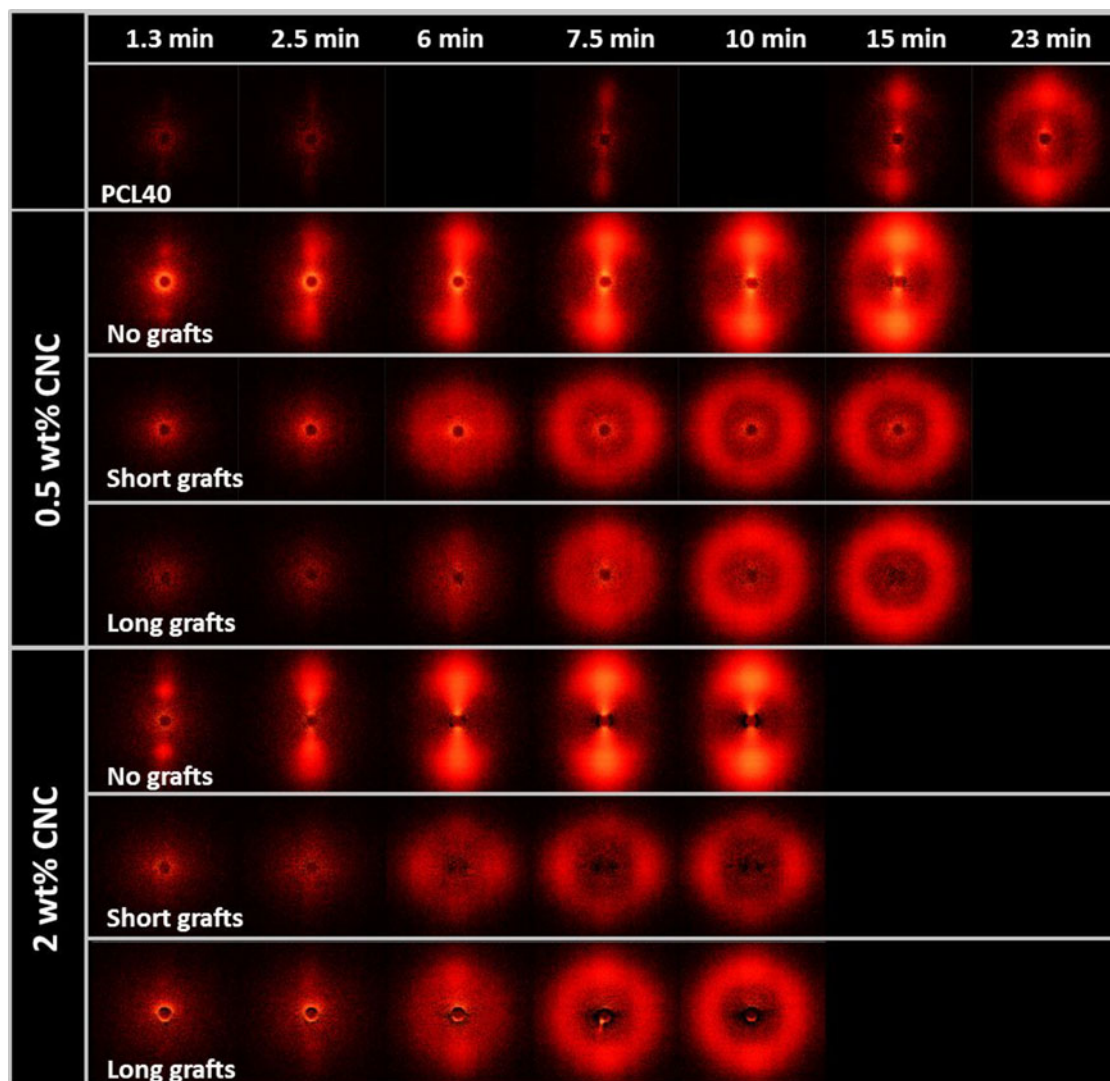


Figure 14. SAXS images obtained during shear-induced crystallization of non-grafted, short grafted and long grafted PCL/CNC nanocomposites. The temperature is 48 °C and the molar mass of the PCL matrix is 40 kg/mol. The shear rate is 60 s^{-1} and the length of the pulse was 1 s.

observed, does not necessarily mean that they are not present, only that their size is smaller than the resolution of the SAXS measurement. This is reasonable, considering the relatively low molar mass of the PCL40 matrix. The influence of molar mass is seen when samples of different molar mass are compared after 3 s of shear. In the PCL80 samples, the chains are longer and do therefore possess longer relaxation times. This accounts for better nucleation and a faster crystallization. The mobility of the longer chains is however limited in the high molar mass matrix, and therefore there is significant isotropic crystallization occurring after the shear is ceased.

In Figure 14 the 2D SAXS images of different composites, obtained after a shear pulse of one second, are presented. It is clear that the fillers have a large influence on shear-induced crystallization. The addition of 0.5 wt% CNC already increases the rate of crystallization significantly. Interestingly, the non-grafted nanocrystals promote the formation of

highly oriented structures with only moderate overgrowth even in the later stages of crystallization, while grafts are disadvantageous for orientation. In the latter case significant isotropic crystallization occurs both in the early and latter stages of crystallization. Increasing the filler content increases the orientation of the oriented structures in the non-grafted samples and leads to the appearance of some orientation in grafted samples, albeit rather modest. Also in this case crystallization is mainly isotropic.

In Figure 15 the 2D SAXS images of different composites, obtained after a longer shear pulse of 3 s, are presented. Similar to the case of short shear pulses, the non-grafted nanocrystals promote the formation of highly oriented structures with moderate overgrowth even in the latter stages of crystallization. The intensity of the meridional lobes is very high, indicating already a high degree of orientation at the early stage of crystallization. In composites with grafted nanocrystals the shear is intense

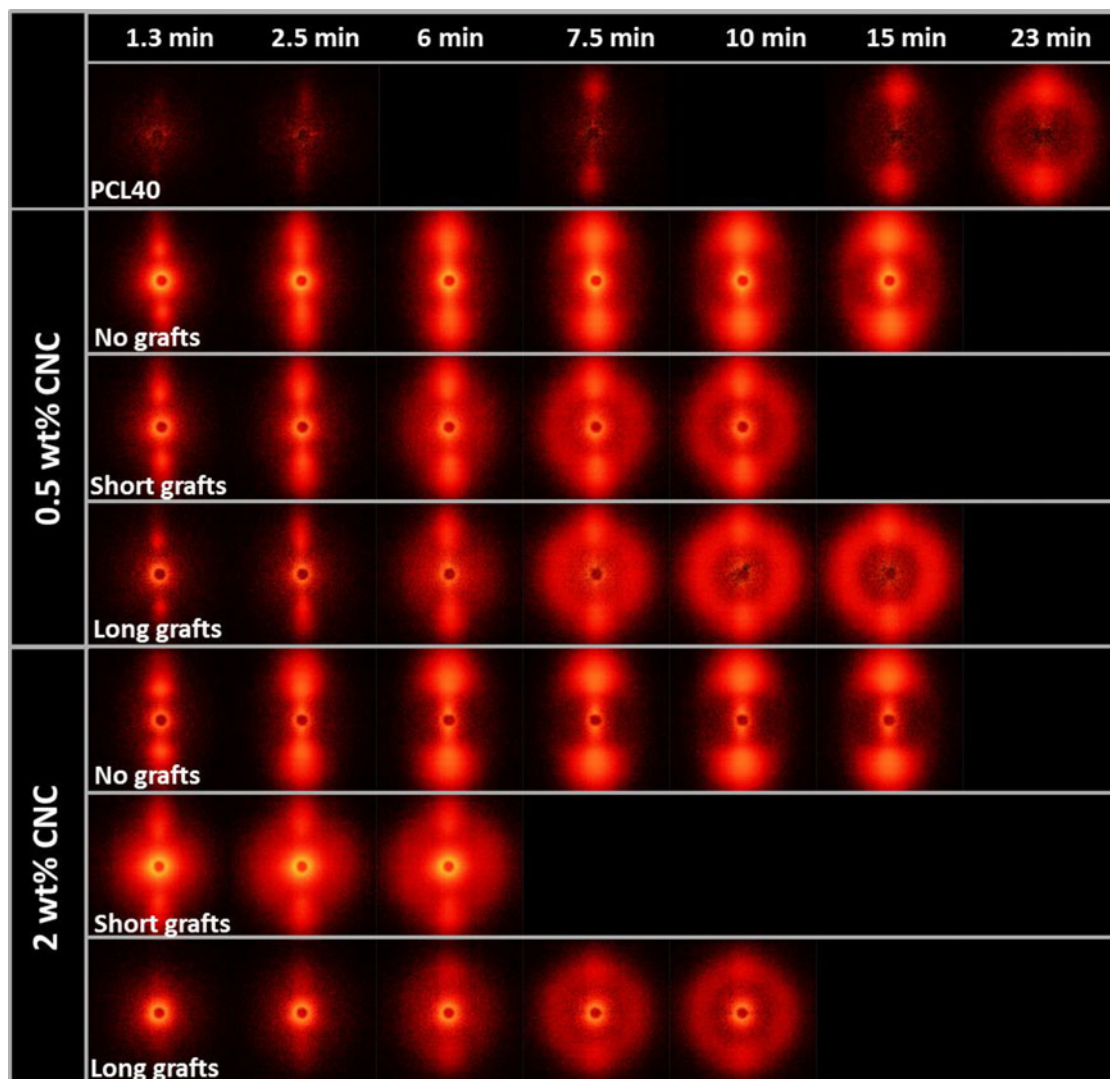


Figure 15. SAXS images obtained during shear-induced crystallization of non-grafted, short grafted and long grafted PCL/CNC nanocomposites. The temperature is 48 °C and the molar mass of the PCL matrix is 40 kg/mol. The shear rate is 60 s^{-1} and the length of the pulse was 3 s.

enough to create some degree of orientation even if significant isotropic crystallization is still occurring in the latter stages of crystallization. The short grafted sample seems to present more orientation than the long grafted. With increasing filler content the intensity of the scattering is increased, which implies a high degree of orientation in the non-grafted samples already at very short times. In the case of short grafted samples the crystallization is clearly accelerated and a mixed mode of crystallization is obtained. For the long grafted samples the orientation appears to be less pronounced than in non-grafted and short grafted samples and a mostly isotropic microstructure is obtained.

As mentioned before, the introduction of fillers can influence the shear-induced crystallization in several ways, especially if the filler is anisotropic and possesses a good nucleation ability. Since the filler can affect both the crystallization behavior and the flow properties of the polymer the understanding of the crystallization behavior is rather complicated.

Starting with the effect of the filler on the flow properties there are two competing effects. The addition of fillers can affect the viscosity of the polymer, and thereby affecting the ‘easiness’ with which chains orient. This implies that the amount of strain that is required to obtain a similar degree of orientation is changed. Moreover the fillers themselves, especially anisotropic fillers, can orient in the direction of the flow, providing templates for oriented crystallization. Filler addition will also affect the relaxation behavior of the polymer chains. Longer relaxation times imply that more row nuclei survive and that crystallization in oriented structures is promoted. In addition to all this, as has already been shown for the quiescent crystallization, the filler is also affecting both the flow-induced nucleation and the subsequent growth of spherulites. Which structure will be dominate depends on the strength of the flow and the molar mass of the polymer. Shear-induced crystallization of a polymer with an anisotropic filler is schematically depicted in [Figure 16](#)

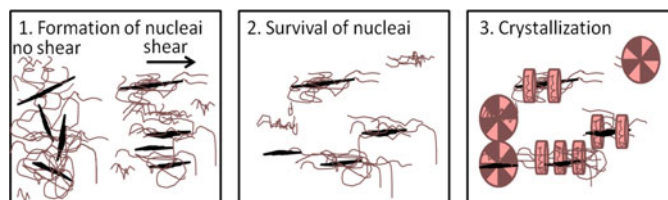


Figure 16. Schematic of the influence of anisotropic fillers on structure development during shear-induced crystallization.

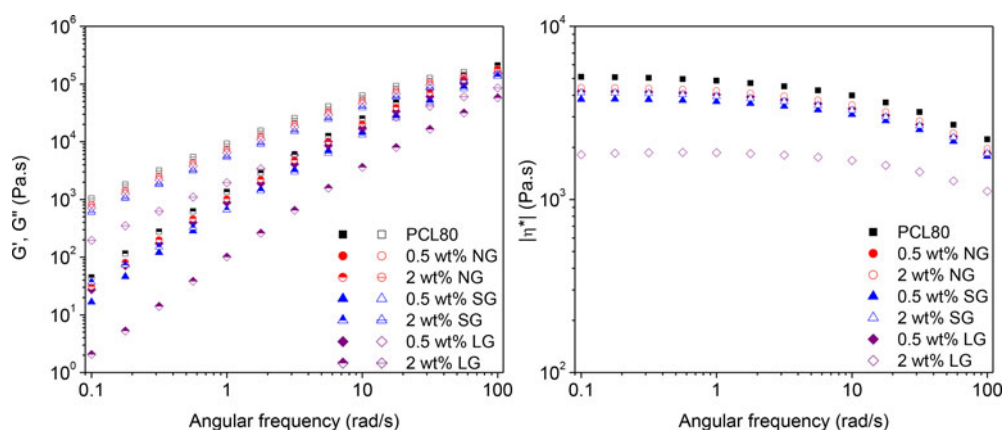


Figure 17. Result from rheological experiments. On the left the loss modulus G'' (open symbols) and storage modulus G' (closed symbols) as a function of angular frequency. On the right the complex viscosity η^* as a function of angular frequency. For all the measurements the temperature was 110°C . The molar mass of the PCL matrix was 80 kg/mol .

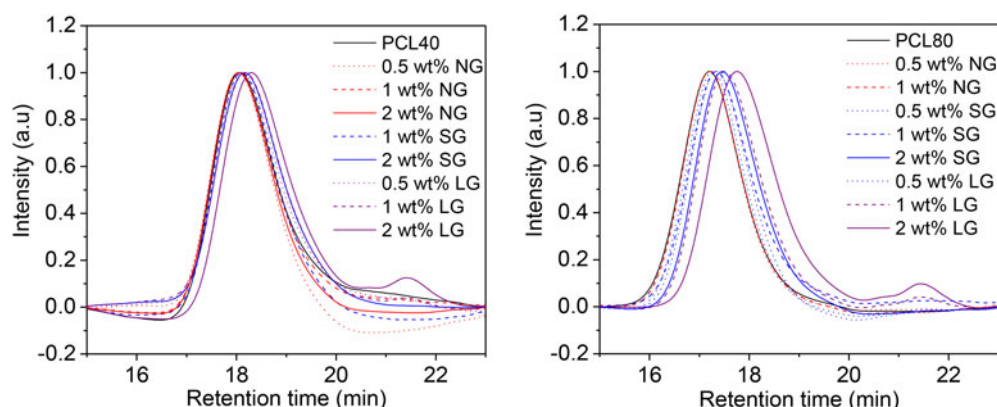


Figure 18. Results from SEC measurements. On the left the results for composites based on PCL40 and on the right the results for PCL80. The samples with non-grafted (NG) fillers are represented by the green curves, short grafted (SG) by the red curves and long grafted (LG) by the blue curves.

and can be summarized as follows: (1) When shear is applied the anisotropic fillers orient in the direction of the shear flow; (2) The chains that are sufficiently oriented will survive and form row nuclei while others will relax and form point-like nuclei; (3) Mixed crystallization takes place, where the abundance of each structure depends on the ratio between row and point-like nuclei.

In all the previous discussions the role of the grafted chains is omitted. However, it is obvious that grafted chains on the filler surface, with a different molar mass than the matrix, further complicate the picture. Not only do these chains affect the rheological behavior of the composite, but they also affect the relaxation behavior, the possibility to orient the polymer in the melt, and the crystallization behavior.

3.3. Rheological behavior of PCL/CNC

In order to better understand the influence of the nanofiller on the shear-induced crystallization the rheological properties of the composites were also investigated. In [Figure 17](#) results from measurements done at 110°C are presented. From these plots it can be concluded that the rheological properties of the melt are rather unaffected by the addition of nanofiller except for samples with a high content of long grafted CNC. In this case a decrease in both the storage (G') and loss (G'') moduli is observed. This result can be explained by the addition of a large portion of PCL with a lower molar mass to the polymer matrix, resulting in a decrease of the overall molar mass of the composite sample and thereby a decrease in melt strength.

In order to confirm this theory, SEC measurements on filtered solutions of the different composites were performed. It has to be pointed out that the solutions were filtered with a $0.2\ \mu\text{m}$ filter before the measurement. This implies that the large clusters visible in the optical microscopy pictures were removed from the solutions, which therefore contained a smaller amount of filler than indicated in the legend. Figure 18 shows the results from the SEC measurements. It can be seen that the addition of non-grafted (NG) fillers or small amounts of grafted fillers has a negligible effect on the molecular weight of the polymer matrix. However, the addition of long grafted (LG) fillers, and large amounts of short grafted (SG) fillers does shift the whole distribution curve towards longer retention times and thus lower molar masses. In the 2 wt% long grafted CNC samples the appearance of a peak at very long retention times confirms the presence of a portion of PCL with a very low molar mass. Although the nanocrystals were washed several times after the grafting reaction it cannot be excluded that this portion of very low molar mass material consists of unreacted monomer. The effect of filler addition on the molar mass distribution is more pronounced in the higher molar mass samples, which is normal given that the difference in molar mass between graft and matrix is much larger in the latter case.

This reduction in molar mass enables us to explain the lower strength and viscosity drop observed in Figure 17. The non-grafted CNC samples show similar viscosities as the neat polymer matrix since we are only adding small amounts of filler. The grafted PCL chains account for a decrease in viscosity at high filler contents due to an increased portion of low molar mass polymer.

Based on these observations the following explanation of the observed shear-induced crystallization behavior of the PCL/CNC nanocomposites can be given:

- Non-grafted CNCs orient in the shear direction and provide templates for oriented crystallization. An increase in shear time results in enhanced orientation with practically all crystalline lamellae oriented perpendicular to the direction of flow. Similar results have been found for polypropylene filled with other anisotropic fillers such as nanoclays [32], carbon nanotubes [35] and graphene [36].
- PCL-g-CNC with short grafts are excellent nucleating agents. However, the grafts hinder orientation of the filler in the direction of flow and therefore mostly point-like nuclei are formed with non-oriented, mainly spherulitic,

crystallization as a result. Stronger flow results in an increased crystallization rate and the formation of a limited amount of oriented structures.

- PCL-g-CNC with long grafts still introduce relatively short chains into a PCL matrix and contribute to an overall lowering of the viscosity of the polymer. Samples which contain a small amount of long grafted CNC exhibit a viscosity which is quite similar to that of the neat polymer. These samples have also a similar rheological behavior to short grafted samples. In the more highly filled samples, the low molar mass of the grafts has an influence on the rheological properties of the matrix, leading to a decrease in viscosity. As a result, the orientation of the polymer chains becomes more difficult and a mainly isotropic structure is found. However, after increasing the shear a limited amount of orientation can be introduced in these samples although the majority of crystallization remains isotropic.

4. Conclusions

Nanocomposites of poly(ϵ -caprolactone) (PCL) with non-grafted cellulose nanocrystals (CNC) and grafted cellulose nanocrystals (PCL-g-CNC) were prepared using melt compounding. These nanocomposite materials did display a very high nucleation ability under quiescent conditions, where especially the grafted nanocrystals showed nucleation efficiencies similar to carbon nanotubes [16,17,19]. Under the influence of shear the non-grafted nanocrystals were however more efficient in orienting in the flow direction, providing templates for oriented crystallization of polymer chains and accelerating the crystallization. PCL-g-CNC with short grafts proved excellent nucleating agents and readily promoted nucleation with or without shear. However, the grafts did hinder orientation of the filler in the direction of flow, leading to mostly non-oriented spherulitic crystallization. The addition of large amounts of grafted material reduced the viscosity of the nanocomposites and through this also the efficiency of shear-induced orientation. Samples containing small amounts of PCL-g-CNC exhibited rheological properties similar to that of the neat polymer.

Acknowledgments

The helpful staff at the DUBBLE beamline at ESRF in Grenoble are greatly acknowledged for their support. The project was funded by the Dutch Polymer Institute (DPI) under project number #623.

Disclosure statement

No potential conflict of interest was reported by the authors.

References

1. Chrissafis K, Antoniadis G, Paraskevopoulos KM, et al. Comparative study of the effect of different nanoparticles on the mechanical properties and thermal degradation mechanism of in situ prepared poly(ϵ -caprolactone) nanocomposites. *Compos Sci Technol.* 2007;67:2165–2174.
2. Di Y, Iannace S, Di Maio E, et al. Nanocomposites by melt intercalation based on polycaprolactone and organoclay. *J Polym Sci B Polym Phys.* 2003;41:670–678.
3. Gorrasi G, Tortora M, Vittoria V, et al. Physical properties of poly(ϵ -caprolactone) layered silicate nanocomposites prepared by controlled grafting polymerization. *J Polym Sci B Polym Phys.* 2004;42:1466–1475.
4. Chen B, Evans JR. Poly(ϵ -caprolactone) – clay nanocomposites: structure and mechanical properties. *Macromolecules* 2006;39:747–754.
5. Luduena LN, Alvarez VA, Vazquez A. Processing and microstructure of PCL/clay nanocomposites. *Mater Sci Eng A.* 2007;460–461:121–129.
6. Fukushima K, Tabuani D, Camino G. Nanocomposites of PLA and PCL based on montmorillonite and sepiolite. *Mate Sci Eng C.* 2009;29:1433–1441.
7. Wu X, Torres FG, Vilaseca F, et al. Influence of the processing conditions on the mechanical properties of chitin crystal reinforced poly(caprolactone) nanocomposites. *J Biobased Mat Bioenergy.* 2007;1:341–350.
8. Habibi Y, Goffin AL, Schiltz N, et al. Bionanocomposites based on poly(ϵ -caprolactone)-grafted cellulose nanocrystals by ring-opening polymerization. *J Mater Chem.* 2008;18:5002–5010.
9. Goffin AL, Raquez JM, Duquesne E, et al. Poly(ϵ -caprolactone) based nanocomposites reinforced by surface-grafted cellulose nanocrystals via extrusion processing: morphology, rheology, and thermomechanical properties. *Polymer* 2011;52:1532–1538.
10. Goffin AL, Habibi Y, Raquez JM, et al. Polyester-grafted cellulose nanocrystals: a new approach for tuning the microstructure of immiscible polyester blends. *ACS Appl Mater Interfaces.* 2012;4:3364–3371.
11. Lönnberg H, Fogelström L, Berglund L, et al. Surface grafting of microfibrillated cellulose with poly(ϵ -caprolactone) – synthesis and characterization. *Eur Polym J.* 2008;44:2991–2997.
12. Lönnberg H, Larsson K, Lindström T, et al. Synthesis of polycaprolactone-grafted microfibrillated cellulose for use in novel bionanocomposites – influence of the graft length on the mechanical properties. *ACS Appl Mater Interfaces.* 2011;3:1426–1433.
13. Siqueira G, Bras J, Dufresne A. Cellulose crystals versus microfibrils: influence of the nature of the nanoparticle and its surface functionalization on the thermal and mechanical properties of nanocomposites. *Biomacromolecules* 2009;10:425–432.
14. Murariu M, Dechief AL, Ramy-Ratiarison R, et al. Recent advances in production of poly (lactic acid)(PLA) nanocomposites: a versatile method to tune crystallization properties of PLA. *Nanocomposites* 2015;1:71–82.
15. Priftis D, Sakellariou G, Hadjichristidis N, et al. Surface modification of multiwalled carbon nanotubes with biocompatible polymers via ring opening and living anionic surface initiated polymerization. Kinetics and crystallization behavior. *J Polym Sci A Polym Chem.* 2009;47:4379–4390.
16. Trujillo M, Arnal ML, Müller AJ, et al. Supernucleation and crystallization regime change provoked by MWNT addition to poly(ϵ -caprolactone). *Polymer* 2012;53:832–841.
17. Mitchell CA, Krishnamoorti R. Non-isothermal crystallization of in situ polymerized poly(ϵ -caprolactone) functionalized-SWNT nanocomposites. *Polymer* 2005;46:8796–8804.
18. Yang Z, Peng H, Wang W, et al. Crystallization behavior of poly(ϵ -caprolactone)/layered double hydroxide nanocomposites. *J Appl Polym Sci.* 2010;116:2658–2667.
19. Chen EC, Wu TM. Isothermal crystallization kinetics and thermal behavior of poly(ϵ -caprolactone)/multi-walled carbon nanotube composites. *Polym Degrad Stab.* 2007;92:1009–1015.
20. Di Maio E, Iannace S, Sorrentino L, et al. Isothermal crystallization in PCL/clay nanocomposites investigated with thermal and rheometric methods. *Polymer* 2004;45:8893–8900.
21. Kumaraswamy G, Issaian AM, Kornfield JA. Shear-enhanced crystallization in isotactic polypropylene. 1. Correspondence between in situ rheo-optics and ex situ structure determination. *Macromolecules* 1999;32:7537–7547.
22. Kumaraswamy G, Kornfield JA, Yeh F, et al. Shear-enhanced crystallization in isotactic polypropylene. 3. Evidence for a kinetic pathway to nucleation. *Macromolecules* 2002;35:1762–1769.
23. Akcora P, Liu H, Kumar SK, et al. Anisotropic self-assembly of spherical polymer-grafted nanoparticles. *Nat Mater.* 2009;8:355–359.
24. Bansal A, Yang H, Li C, et al. Controlling the thermomechanical properties of polymer nanocomposites by tailoring the polymer-particle interface. *J Polym Sci B Polym Phys.* 2006;44:2944–2950.
25. Zhou B, Tong ZZ, Huang J, et al. Isothermal crystallization kinetics of multi-walled carbon nanotubes-graft-poly(ϵ -caprolactone) with high grafting degrees. *CrystEngComm* 2013;15:7824–7832.
26. Eichhorn SJ, Dufresne A, Aranguren M, et al. Current international research into cellulose nanofibres and nanocomposites. *J Mater Sci.* 2010;45:1–33.
27. Samain X, Langlois V, Renard E, et al. Grafting biodegradable polyesters onto cellulose. *J Appl Polym Sci.* 2011;121:1183–1192.
28. Goffin AL, Raquez JM, Duquesne E, et al. From interfacial ring-opening polymerization to melt processing of cellulose nanocrystal-filled polylactide-based nanocomposites. *Biomacromolecules* 2011;12:2456–2465.
29. Fillon B, Wittmann JC, Lotz B, et al. Self-nucleation and recrystallization of isotactic polypropylene (α phase) investigated by differential scanning calorimetry. *J Polym Sci B Polym Phys.* 1993;31:1383–1393.

30. Fillon B, Lotz B, Thierry A, et al. Self-nucleation and enhanced nucleation of polymers. Definition of a convenient calorimetric “efficiency scale” and evaluation of nucleating additives in isotactic polypropylene (α phase). *J Polym Sci B Polym Phys*. 1993;31:1395–1405.
31. Dikovskiy D, Marom G, Avila-Orta CA, et al. Shear-induced crystallization in isotactic polypropylene containing ultra-high molecular weight polyethylene oriented precursor domains. *Polymer* 2005;46:3096–3104.
32. Rozanski A, Monasse B, Szkudlarek E, et al. Shear-induced crystallization of isotactic polypropylene based nanocomposites with montmorillonite. *Eur Polym J*. 2009;45:88–101.
33. Patil N, Balzano L, Portale G, et al. Influence of shear in the crystallization of polyethylene in the presence of SWCNTs. *Carbon* 2010;48:4116–4128.
34. Sun T, Chen F, Dong X, et al. Shear-induced orientation in the crystallization of an isotactic polypropylene nanocomposite. *Polymer* 2009;50:2465–2471.
35. Chen YH, Zhong GJ, Lei J, et al. In situ synchrotron X-ray scattering study on isotactic polypropylene crystallization under the coexistence of shear flow and carbon nanotubes. *Macromolecules* 2011;44:8080–8092.
36. Xu JZ, Chen C, Wang Y, et al. Graphene nanosheets and shear flow induced crystallization in isotactic polypropylene nanocomposites. *Macromolecules* 2011;44:2808–2818.